BRAZILIAN JOURNAL
OF MEDICAL AND BIOLOGICAL RESEARCH
www.bjournal.com.br

ISSN 0100-879X
Volume 43 (12) 1135-1244 December 2010

BIOMEDICAL SCIENCES
AND
CLINICAL INVESTIGATION

Braz J Med Biol Res, December 2010, Volume 43(12) 1203-1214

doi: 10.1590/S0100-879X2010007500125

Proteomic analysis of cytosolic proteins associated with petite mutations in Candida glabrata

C.V. Loureiro y Penha, P.H.B. Kubitschek, G. Larcher, J. Perales, I. Rodriguez León, L.M. Lopes-Bezerra and J.P. Bouchara

Brazilian Journal of Medical and Biological Research (2010) 43: 1203-1214
ISSN 0100-879X

Proteomic analysis of cytosolic proteins associated with petite mutations in *Candida glabrata*

C.V. Loureiro y Penha[1], P.H.B. Kubitschek[1], G. Larcher[2], J. Perales[3], I. Rodriguez León[3], L.M. Lopes-Bezerra[1] and J.P. Bouchara[2]

[1]Laboratório de Micologia Celular e Proteômica, Instituto de Biologia Roberto Alcântara Gomes, Universidade do Estado do Rio de Janeiro, Rio de Janeiro, RJ, Brasil
[2]Host-Parasite Interaction Study Group, UPRES-EA 3142, Laboratory of Parasitology-Mycology, Angers University Hospital, Angers, France
[3]Laboratório de Toxinologia, Instituto Oswaldo Cruz, Fiocruz, Rio de Janeiro, RJ, Brasil

Abstract

The incidence of superficial or deep-seated infections due to *Candida glabrata* has increased markedly, probably because of the low intrinsic susceptibility of this microorganism to azole antifungals and its relatively high propensity to acquire azole resistance. To determine changes in the *C. glabrata* proteome associated with petite mutations, cytosolic extracts from an azole-resistant petite mutant of *C. glabrata* induced by exposure to ethidium bromide, and from its azole-susceptible parent isolate were compared by two-dimensional polyacrylamide gel electrophoresis. Proteins of interest were identified by peptide mass fingerprinting or sequence tagging using a matrix-assisted laser desorption/ionization tandem time-of-flight mass spectrometer. Tryptic peptides from a total of 160 Coomassie-positive spots were analyzed for each strain. Sixty-five different proteins were identified in the cytosolic extracts of the parent strain and 58 in the petite mutant. Among the proteins identified, 10 were higher in the mutant strain, whereas 23 were lower compared to the parent strain. The results revealed a significant decrease in the enzymes associated with the metabolic rate of mutant cells such as aconitase, transaldolase, and pyruvate kinase, and changes in the levels of specific heat shock proteins. Moreover, transketolase, aconitase and catalase activity measurements decreased significantly in the ethidium bromide-induced petite mutant. These data may be useful for designing experiments to obtain a better understanding of the nuclear response to impairment of mitochondrial function associated with this mutation in *C. glabrata*.

Key words: *Candida glabrata*; Petite mutations; Cytosolic extracts; Proteomic analysis; Azole resistance

Introduction

The incidence of life-threatening fungal infections that are mainly caused by the *Candida* species has increased dramatically in the past decades along with the development of antibiotic treatments, the widespread use of immunosuppressive therapy, and the emergence of the AIDS epidemic (1). Among the causative agents of these infections, *Candida albicans* remains by far the most frequent, but infections due to other *Candida* species are being reported increasingly (2,3). For instance, *C. glabrata* has recently emerged as a significant pathogen in various hospital settings, where it is responsible for an increasing number of systemic infections and candiduria (4,5). In a recent study conducted in the United States, *C. glabrata* ranked second among the causative agents of fungemia, accounting for 21% of all *Candida* bloodstream isolates (6,7). The rise in the number of *C. glabrata* systemic infections is due to the poor intrinsic susceptibility of this yeast to azole antifungals and to its propensity to acquire azole resistance (5,8-12).

The mechanisms of resistance to azole antifungals have been studied mainly in *C. albicans* and can be categorized as i) changes in the cell wall or plasma membrane, which lead to impaired azole uptake; ii) alterations in the affinity of azoles for their target Erg11p (lanosterol 14α-demethylase) or increase in the cellular content of Erg11p due to mutations in or overexpression of the *ERG11* gene, respectively, and iii) increased efflux of the azole drugs mediated by

Correspondence: C.V. Loureiro y Penha, LMCProt, IBRAG, UERJ, Rua São Francisco Xavier, 524, PHLC 501-D, 20550-013 Rio de Janeiro, RJ, Brasil. Fax: +55-21-2587-7377. E-mail: carlapenha@hotmail.com

Received December 10, 2009. Accepted October 21, 2010. Available online November 12, 2010. Published December 20, 2010.

membrane transport proteins belonging to the ATP-binding cassette (ABC) transporter family (*CDR1* and *CDR2*) or to the major facilitator superfamily (*MDR1* and *FLU1*). For instance, the *CDR1*, *CDR2* and *MDR1* genes have been shown to be overexpressed in many azole-resistant isolates, and deletion of these genes resulted in hypersensitivity to azoles (13). However, different mechanisms including overexpression of genes encoding the efflux pumps and overexpression or point mutations in the *ERG11* gene frequently combine, resulting in a stepwise development of azole resistance over time (14). In addition, compensatory pathways that involve alterations of specific steps in ergosterol biosynthesis have been documented as resistance mechanisms to both azoles and polyene antifungals (15).

More recently, increased levels of expression of the ABC transporter genes *C. glabrata CDR1* (*CgCDR1*) and *CDR2* (*CgCDR2*) were detected in azole-resistant isolates of *C. glabrata* (16-18). Furthermore, the azole resistance of *C. glabrata* petite mutants obtained by exposure to fluconazole or induced by ethidium bromide (ETB) was shown to be associated with the up-regulation of the nuclear genes *CgCDR1* and *CgCDR2* (19,20). However, due to the numerous cross-talks between the nucleus and mitochondria, petite mutations may also lead to the deregulation of the expression of other nuclear genes (21). For instance, an increased cellular content of free ergosterol due to a defect in sterol esterification has been reported in petite mutants (19). Similarly, changes in the biochemical composition of the cell wall associated with a lower cell surface hydrophobicity were also observed in mutant cells, as well as an increased expression of the *CgEPA1* gene encoding a lectin involved in adherence to epithelial cells (22).

In the present study, changes in the *C. glabrata* proteome associated with petite mutations and azole resistance were examined by investigation of an azole-susceptible wild-type isolate and an ETB-induced azole-resistant petite mutant.

Material and Methods

Yeast strains and culture conditions

The study was carried out using a *C. glabrata* clinical isolate designated 90.1085, which was obtained at the Laboratory of Parasitology and Mycology of Angers University Hospital, Angers, France, from a urine sample collected in 1990, and a derived petite mutant induced by exposure to the intercalating agent ETB (Sigma-Aldrich, USA). The mutant presented cross-resistance to azoles due to overexpression of the *CDR1* and *CDR2* genes. The parent isolate and its ETB-induced petite mutant were maintained by biweekly passages in yeast extract-peptone-glucose (YEPD) agar containing 5 g/L yeast extract, 10 g/L peptone, 20 g/L glucose, 0.5 g/L chloramphenicol, and 20 g/L agar. Mutant cells were subcultured on yeast extract-peptone agar containing 2% glycerol as the sole carbon source to ascertain their respiratory deficiency. Both isolates were preserved in 20% glycerol at -80°C.

Cytosolic protein extraction

For the isolation of cytosolic proteins, blastoconidia were washed in deionized distilled water and resuspended in 10 mM Tris-HCl, pH 7.4, containing 300 U RNase and a mix of protease inhibitors (1 mM phenylmethylsulfonyl fluoride, 1 mM ethylenediamine tetraacetic acid and 1 µM pepstatin). Cells were disrupted using glass beads in a Braun homogenizer with cooling CO_2 and the suspensions obtained were centrifuged at 12,000 *g* for 30 min at 4°C. The pellets were discarded, and the supernatants were centrifuged for 1 h at 75,000 *g*. The resulting supernatants, which correspond to the cytosolic extracts, were desalted by dialysis and protein content was measured using the Bradford (Bio-Rad Laboratories, USA) and the BCA protein assay kit (Thermo Scientific, USA).

2-D SDS-PAGE

Samples containing 150 µg (analytical gels) or 500 µg (preparative gels) protein were solubilized in a lysis buffer consisting of 7 M urea, 2 M thiourea, 4% CHAPS, 64 mM dithioerythritol, 0.5% Pharmalyte, pH 3-11 (Amersham Biosciences, Sweden) and bromophenol blue and then applied onto Immobiline, pH 3-11, nonlinear DryStrips (18 cm long; Amersham Biosciences). Isoelectric focusing was performed using an IPGphor system (Amersham Biosciences) at 20°C and the following program: 30 V (active rehydration) for 12 h, 200 V for 1 h, 500 V for 1 h, 500-10,000 V for 3 h, and 10,000 V for 1 h. Immobilized pH gradient strips were then reduced (1% dithioerythritol) and alkylated (1.5% iodoacetamide) in equilibration buffer (6 M urea, 75 mM Tris-HCl, pH 8.8, 29.3% glycerol, 2% SDS) (23). The second dimension run was performed in homogeneous 12% polyacrylamide slab gels (1.5 mm thick) at 5 mA for 30 min, 8 mA for 1 h and 60 mA for 4 h using a Protean II electrophoresis apparatus (Bio-Rad).

For the determination of the total number of spots, analytical gels were silver-stained as described by Bjellqvist et al. (24), fixed first in methanol-acetic acid-distilled water (4:1:5) for 1 h and then in ethanol-acetic acid-distilled water (0.5:0.5:9) overnight. The gels were rinsed with 7.5% acetic acid and incubated in 1% glutaraldehyde containing 0.5 M sodium acetate for 30 min. The gels were then extensively washed with water and stained with an ammoniacal silver nitrate solution for 30 min. Gels were washed and color was developed in 0.01% citric acid containing 0.1% formaldehyde. Staining was stopped with 5% Tris in 2% acetic acid.

Preparative gels for further analysis of proteins by mass spectrometry were stained with colloidal Coomassie blue R-250 (Bio-Rad). The gels were destained using several changes of distilled water over a 2-h period. Finally, spots were excised and in gel-digested for analysis by matrix-assisted laser desorption/ionization tandem time-of-flight mass spectrometry (MALDI-TOF/TOF MS).

Image analysis

Silver- and Coomassie-stained gels were captured with an Image Scanner (Amersham Biosciences). Different 2-D

images were processed for detection, volumetric quantification, matching, and editing of molecular masses and pI of spots, using ImageMaster 2-D Platinum software (Amersham Biosciences). Proteins were considered to be differentially increased or decreased if the protein spot in the ETB-induced mutant showed statistically significant differences of 2-fold or more in their mean spot volume on at least three of four gels ($P < 0.05$, *t*-test) compared to its parent isolate.

In-gel tryptic digestion

Digestion was performed by the method of Pitarch et al. (25). Protein spots were excised from Coomassie-stained 2-D gels and transferred to 0.5-mL tubes. Gel fragments were destained with acetonitrile (ACN), washed twice with 50% ACN in 25 mM ammonium bicarbonate (AmBic), and vacuum-dried. The proteins were then reduced with 10 mM dithioerythritol in 25 mM AmBic for 30 min at 56°C and subsequently alkylated with 55 mM iodoacetamide in 25 mM AmBic for 20 min in the dark. Next, the gel fragments were washed with 25 mM AmBic and ACN and dried under vacuum. All gel fragments were incubated with 12.5 ng/µL sequencing grade trypsin (Promega, USA) in 25 mM AmBic overnight at 37°C. Peptides were then extracted from the gel fragments with 50% ACN, 1% trifluoroacetic acid in 25 mM AmBic, and finally with 100% ACN. The extracts were pooled, and concentrated by evaporation of the solvent with a SpeedVac apparatus (Thermo Fisher Scientific, USA).

MALDI-TOF/TOF MS

Peptides were applied onto a MALDI plate after co-crystallization with and α-cyano 4-hydroxycinnamic acid (CHCH) matrix (Sigma-Aldrich). One microliter of each sample with 0.4 µL 3 mg/mL CHCH matrix in 50% ACN and 0.01% trifluoroacetic acid was spotted onto a MALDI plate. MS/MS sequencing analyses were carried out using a MALDI-TOF/TOF MS 4700 Proteomics Analyzer (Applied Biosystems, USA).

Database search

Peak lists from all MS/MS spectra were submitted to a database search using an in-house copy of MASCOT, version 3.1 (Matrix Science Inc., USA). The following criteria were used for all database searches: a minimum signal-to-noise ratio threshold of 5-10; mass values in the 0-60 Da range and masses within 20 Da of the precursor ion mass were excluded. A maximum of 60 peaks per spectrum were included as product ions. The mass tolerance was ±75 ppm for MS data, ±200 ppm for MS/MS precursor ions, and ±250 ppm for MS/MS product ions. The sample was searched against the NCBInr database (October 4, 2007). The ExPASy (Expert Protein Analysis System) proteomics server of the Swiss Institute of Bioinformatics (SIB) was used for the analysis of protein sequences.

Measurements of transketolase and aconitase activity

To estimate the transketolase activity, samples were added to a cuvette containing buffer (50 mM Tris-HCl, pH 7.6), 2 mM ribose 5-phosphate, 1 mM xylulose 5 phosphate, 5 mM $MgCl_2$, 0.2 U/mL triosephosphate isomerase, 0.2 mM NADH, and 0.1 mM thiamine pyrophosphate. Reactions were initiated by the addition of cytosolic extracts at 37°C. The aconitase activity was determined by addition of the samples to a cuvette containing buffer (50 mM Tris-HCl, pH 7.4), 0.6 mM $MnCl_2$, and 0.5 mM ferrous ammonium sulfate. Reactions were initiated by the addition of cytosolic extracts at 37°C. Transketolase and aconitase activities were measured by spectrophotometry (340 nm) (Thermo Spectronic Genesys 10 uv), and data are reported as ng product·min^{-1}·mg total protein^{-1}. Total protein content of cytosolic extracts was determined by the method of Bradford. Each experiment was repeated three times.

Measurements of catalase activity

Catalase activity was measured by the method of Aebi (26), which is based on the principle that the absorbance will decrease due to dismutation of H_2O_2 at 240 nm (UV-visible spectrophotometry). The amount of H_2O_2 converted into H_2O and oxygen in 1 min under standard conditions is accepted as enzyme reaction velocity. Data are reported as µmol H_2O_2 metabolized·min^{-1}·mg total protein^{-1}.

Statistical analysis

Statistical analysis for the enzyme activity data was performed using the Student *t*-test, with the level of significance set at $P < 0.05$. For identification of protein, the Mascot protein score reports a match as significant if it has a match with less than 5% chance of being a random hit. Protein scores are derived from ion scores as a non-probabilistic basis for ranking protein hits. Protein score is -10*Log(P), where P is the probability that the observed match is a random event. Individual protein scores >50 indicate identity or extensive homology ($P < 0.05$).

Results

In order to identify differences in protein expression between the parent isolate and its derived petite mutant, differences in protein profiles between cytosolic protein extracts from cultures of the two isolates were examined. Equal amounts of each protein extract (parent isolate and ETB-induced petite mutant) were submitted to 2-D electrophoresis. Multiple gels from three independent experiments were run for each sample to ascertain reproducibility. One representative gel of each extract was used as a reference 2-D map (Figure 1). Analysis of the virtual image generated using the ImageMaster Platinum software and based on the overlay of the reference 2-D maps permitted the observation of significant differences in the protein pattern between the two isolates (Figure 2). In the silver-stained 2-D gels, 664 and 626 spots were visualized for the parent isolate and its ETB-induced petite mutant, respectively (data not shown). Although lower numbers of spots were observed on the Coomassie-stained gels, 364 in the parent isolate and 326 in the ETB-induced petite mutant, the main differences remained the same as expected (Figure 2).

For protein identification, the spots were digested in-gel and analyzed by MALDI-TOF/TOF MS. Bioinformatic analysis of MALDI-TOF spectra permitted the identification of a total of 65 different proteins in the parent isolate and 58 in the ETB-induced petite mutant corresponding to the 140 and 121 spots, respectively, numbered in Figure 1. A list of identified proteins is presented in Table 1, together with their accession numbers, peptides matched, sequence

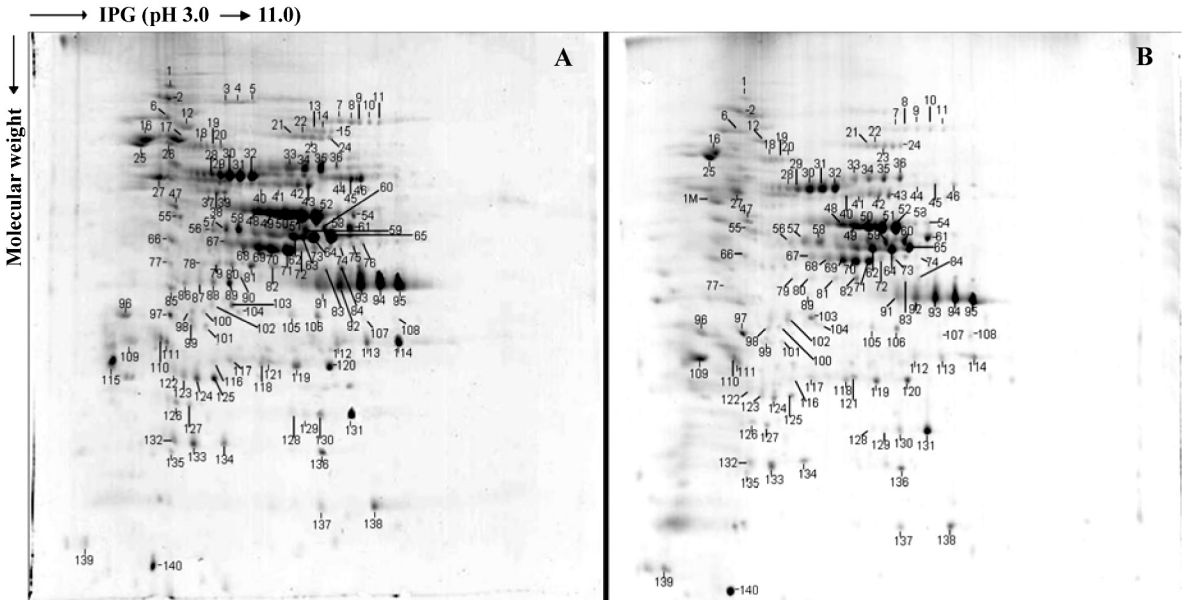

Figure 1. 2-D gels of cytoplasmic protein extracts of the *Candida glabrata* parent isolate and its ethidium bromide (ETB)-induced petite mutant separated on immobilized pH gradient (IPG) strips covering the pH range of 3 to 11. The gels were stained with colloidal Coomassie blue. *A*, Parent isolate; *B*, ETB-induced petite mutant. The protein spots that were identified are numbered and listed in Table 1.

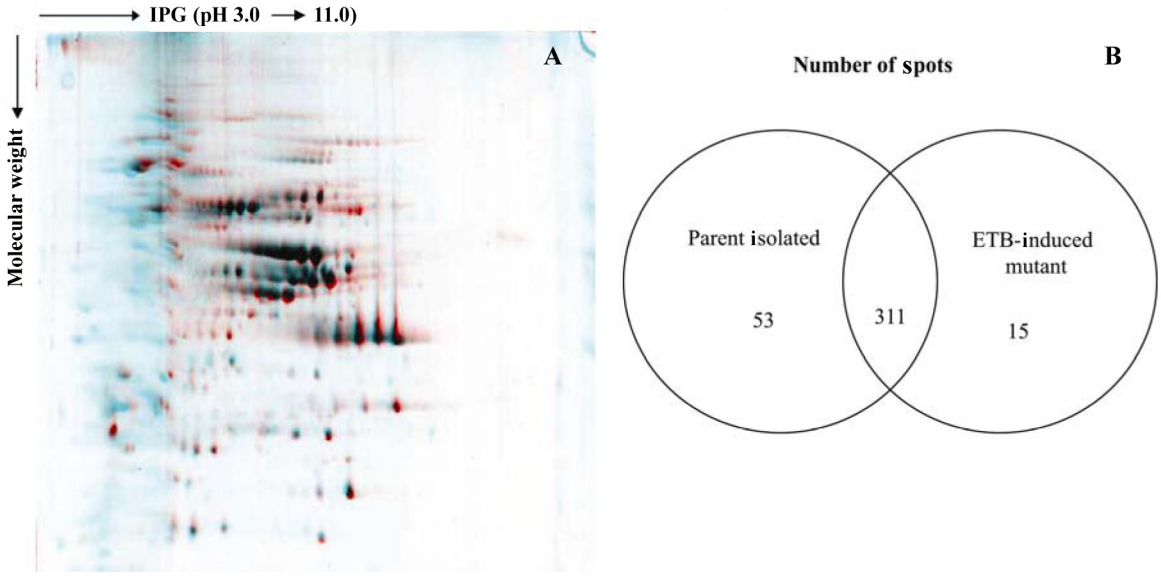

Figure 2. Two-dye overlay (parent isolate/ethidium bromide (ETB)-induced petite mutant). *A*, Virtual image generated using the ImageMaster Platinum software and based on the overlay from 2-D maps of *Candida glabrata* isolates where the blue spots indicate the ETB-induced petite mutant, and the red spots, the parent isolate. *B*, Venn's diagram presenting the total number of spots visualized in each 2-D map. IPG = immobilized pH gradient.

Table 1. Proteins identified by two-dimensional sodium dodecyl sulfate-polyacrylamide gel electrophoresis and matrix-assisted laser desorption/ionization tandem time-of-flight mass spectrometry.

Spot	Accession number[a]	Peptides matched	Sequence coverage (%)	Score[b]	Protein (description)[c]	Fold change[d]
1	Q6FTB5	4	6.9	71	Ubiquitin-activating enzyme	1.70
2	Q6FNS8	5	12.2	88	AAA ATPases family/cell division protein 48	0.89
3	Q6FNS8	4	5.3	73	Heat shock protein 104	P[e]
4	Q6FTB3	4	5.3	73	Heat shock protein 104	P
5	Q6FTB3	4	5.3	73	Heat shock protein 104	P
6	Q6BSA2	5	13.8	134	Heat shock protein 90	1.98
7	Q6FVR0	5	9.8	86	Aconitase	2.68
8	Q6FVR0	5	9.8	86	Aconitase	3.71
9	Q6FVR0	5	9.8	86	Aconitase	2.59
10	Q6FVR0	5	9.8	86	Aconitase	1.78
11	Q6FVR0	5	9.8	86	Aconitase	2.90
12	Q6FJI3	4	8.7	93	Heat shock protein homolog SSE1	0.99
13	Q6FLU2	4	10.5	121	Acetyl-coenzyme A synthetase 1	P
14	Q6FLU2	4	10.5	121	Acetyl-coenzyme A synthetase 1	P
15	Q6FLU2	4	10.5	121	Acetyl-coenzyme A synthetase 1	P
16	Q6FTD8	6	13.8	201	Heat shock protein 70	1.82
17	Q6FTD8	6	13.8	201	Heat shock protein 70	P
18	Q876N3	4	9.2	164	Heat shock protein SSB	1.51
19	Q876N3	6	12.6	172	Heat shock protein SSB	0.83
20	Q876N3	6	12.6	172	Heat shock protein SSB	1.00
21	Q6FWC3	6	15.9	162	Transketolase	1.03
22	Q6FWC3	6	15.9	162	Transketolase	1.72
23	Q6FWC3	6	15.9	162	Transketolase	0.98
24	Q6FWC3	6	15.9	162	Transketolase	2.69
25	Q6FTB5	4	12.0	188	Heat shock protein 70	0.51
26	Q6FMR2	4	11.4	152	Chaperonin (heat shock protein 60)	P
27	Q6FM56	5	16.4	212	Catalase A	0.95
28	Q6FJA3	4	9.6	94	Pyruvate decarboxylase	0.99
29	Q6FJA3	4	9.6	94	Pyruvate decarboxylase	0.89
30	Q6FJA3	4	9.6	94	Pyruvate decarboxylase	0.96
31	Q6FJA3	5	12.2	129	Pyruvate decarboxylase	0.66
32	Q6FJA3	6	14.6	134	Pyruvate decarboxylase	0.64
33	Q6FIS9	6	16.8	194	Pyruvate kinase 1	3.18
34	Q6FIS9	6	16.8	194	Pyruvate kinase 1	2.57
35	Q6FIS9	6	16.8	194	Pyruvate kinase 1	3.55
36	Q6FIS9	6	16.8	194	Pyruvate kinase 1	1.11
37	Q6FUU4	5	12.7	188	Hexokinase	P
38	Q6FUU4	5	12.7	188	Hexokinase	P
39	Q6FUU4	5	12.7	188	Hexokinase	P
40	Q6FVB8	5	13.8	216	Cystathionine beta-synthase domain pair family	0.4
41	Q6FP06	5	16.0	316	Glucose-6-phosphate 1-dehydrogenase	1.65
42	Q6FRW1	5	14.6	316	Glucose-6-phosphate isomerase	1.12
43	Q6FRW1	5	14.6	316	Glucose-6-phosphate isomerase	1.70
44	Q6FM56	6	15.6	274	Catalase	3.61
45	Q6FM56	6	15.6	274	Catalase	2.66
46	Q6FM56	6	15.6	274	Catalase	3.19
47	Q6FSH4	7	19.9	414	ATP synthase beta subunit	2.82

Continued on next page

Table 1 continued

Spot	Accession number[a]	Peptides matched	Sequence coverage (%)	Score[b]	Protein (description)[c]	Fold change[d]
48	Q6FQY4	5	20.6	275	Enolase 2	0.78
49	Q6FQY4	5	20.6	275	Enolase 2	1.32
50	Q6FQY4	6	23.3	298	Enolase 2	1.12
51	Q6FQY4	7	26.1	302	Enolase 2	1.04
52	Q6FQY4	6	23.3	298	Enolase 2	1.00
53	Q6FIM1	6	15.3	155	6-Phosphogluconate dehydrogenase	2.35
54	Q6FIM1	6	15.3	155	6-Phosphogluconate dehydrogenase	2.61
55	Q6FQQ6	5	21.5	406	ATP-dependent RNA helicase eIF4A	0.37
56	Q6FXL1	4	16.6	351	S-adenosylmethionine synthetase	0.33
57	P60009	5	18.4	155	Actin	0.52
58	P60009	5	18.4	155	Actin	0.67
59	Q6FKY1	6	20.0	207	Phosphoglycerate kinase	0.64
60	Q6FKY1	6	20.0	207	Phosphoglycerate kinase	0.59
61	Q6FKY1	6	20.0	207	Phosphoglycerate kinase	0.89
62	Q6FQA4	5	22.2	385	Alcohol dehydrogenase	0.62
63	Q6FQA4	5	22.2	385	Alcohol dehydrogenase	P
64	Q6FQA4	5	22.2	385	Alcohol dehydrogenase	0.94
65	Q6FQA4	6	28.7	341	Alcohol dehydrogenase	0.67
66	Q6FWJ7	5	16.1	232	Glycerol-3-phosphate dehydrogenase 2	0.57
67	Q6FLL5	5	22.2	288	Fructose-bisphosphate aldolase	0.57
68	Q6FLL5	5	22.2	288	Fructose-bisphosphate aldolase	0.55
69	Q6FLL5	5	22.2	288	Fructose-bisphosphate aldolase	0.99
70	Q6FLL5	7	27.2	252	Fructose-bisphosphate aldolase	0.97
71	Q6FLL5	7	27.2	252	Fructose-bisphosphate aldolase	1.63
72	Q6FV31	3	18.5	178	NAD-dependent epimerase/dehydratase	1.71
73	Q6FV31	3	18.5	178	NAD-dependent epimerase/dehydratase	1.69
74	Q6FQD0	5	24.7	367	Isocitrate dehydrogenase	0.85
75	Q6FL28	4	14.1	104	Flavohemoglobin	P
76	Q6FL28	3	8.3	96	Flavohemoglobin	P
77	Q6FKT0	4	16.0	115	Unnamed protein product	1.31
78	Q6FXG5	4	14.7	146	Transaldolase	2.95
79	Q6FXG5	4	14.7	146	Transaldolase	2.87
80	Q6FXG5	5	18.3	176	Transaldolase	2.53
81	Q6FXG5	6	22.8	188	Transaldolase	1.57
82	Q6FXG5	5	18.3	176	Transaldolase	0.85
83	Q6FSM4	3	16.2	118	Glyceraldehyde-3-phosphate dehydrogenase 2	1.81
84	Q6FSM4	3	16.2	118	Glyceraldehyde-3-phosphate dehydrogenase 2	2.41
85	Q6FMM4	4	20.4	261	Transketolase	P
86	Q6FRB7	3	18.8	204	Inorganic pyrophosphatase	P
87	Q6FPW3	5	16.3	123	Glyceraldehyde-3-phosphate dehydrogenase 1	P
88	Q6FPW3	5	16.3	123	Glyceraldehyde-3-phosphate dehydrogenase 1	P
89	Q6FPW3	7	32.5	154	Glyceraldehyde-3-phosphate dehydrogenase 1	0.15
90	Q6FMY5	4	16.3	117	Transaldolase	P
91	Q6FSM4	4	25.3	188	Glyceraldehyde-3-phosphate dehydrogenase 2	2.15
92	Q6FSM4	6	31.9	191	Glyceraldehyde-3-phosphate dehydrogenase 2	1.62
93	Q6FSM4	7	38.9	223	Glyceraldehyde-3-phosphate dehydrogenase 2	1.29
94	Q6FSM4	7	38.9	223	Glyceraldehyde-3-phosphate dehydrogenase 2	1.10
95	Q6FSM4	7	38.9	223	Glyceraldehyde-3-phosphate dehydrogenase 2	1.11
96	Q6FTV4	4	38.2	214	Eukaryotic elongation factor 1 guanine nucleotide exchange	1.01

Continued on next page

Table 1 continued

Spot	Accession number[a]	Peptides matched	Sequence coverage (%)	Score[b]	Protein (description)[c]	Fold change[d]
97	Q6FJX4	5	25.5	351	Ribosomal protein S2	0.51
98	Q6FN26	4	14.8	112	Aldose 1-epimerase	0.72
99	Q6FX79	3	17.6	123	Phosphatidylethanolamine-binding protein	1.99
100	Q6FN26	4	23.6	186	Aldose 1-epimerase	1.06
101	Q6FMG7	4	11.5	89	Cytochrome C peroxidase	1.29
102	Q6FW89	4	27.8	314	WD domain, G-beta repeat family	0.31
103	Q6FW89	4	27.8	314	WD domain, G-beta repeat family	0.39
104	Q6FWB8	4	20.8	251	Spermine/spermidine synthase family	1.44
105	Q6FQI9	5	27.5	255	Haloacid dehalogenase-like hydrolase	1.42
106	Q6FQI9	6	34.0	416	Haloacid dehalogenase-like hydrolase	1.04
107	Q6FXR3	2	16.2	233	Flavodoxin	0.14
108	Q6FXR3	2	16.2	233	Flavodoxin	0.22
109	Q6FUX8	4	23.5	154	Phosphoglycerate mutase	0.12
110	Q6FKF2	5	28.8	233	14-3-3 protein family	0.15
111	Q6FKF2	5	28.8	233	14-3-3 protein family	0.31
112	Q6FUX8	4	24.7	298	Phosphoglycerate mutase	3.00
113	Q6FUX8	4	24.7	298	Phosphoglycerate mutase	2.52
114	Q6FUX8	5	32.4	404	Phosphoglycerate mutase	2.76
115	Q6FUZ5	4	50.0	333	Unnamed protein product	P
116	Q6FLR5	3	14.7	184	Haloacid dehalogenase-like hydrolase	0.89
117	Q6FLR5	4	24.7	197	Haloacid dehalogenase-like hydrolase	0.79
118	Q6FRI3	5	23.4	155	Triosephosphate isomerase	1.08
119	Q6FRI3	5	23.4	155	Triosephosphate isomerase	1.16
120	Q6FRI3	6	29.4	276	Triosephosphate isomerase	1.23
121	Q6FM32	4	23.4	271	Adenylate kinase	1.51
122	Q6FX51	4	25.0	112	DJ-1/PfpI family	4.91
123	Q6FX51	5	33.9	123	DJ-1/PfpI family	1.51
124	Q6FX51	4	25.0	112	DJ-1/PfpI family	1.71
125	Q6FX51	6	41.1	298	DJ-1/PfpI family	1.22
126	Q6FSW7	5	39.0	367	NADH dehydrogenase	0.84
127	Q6FSW7	5	39.0	367	NADH dehydrogenase	0.57
128	Q6FM13	2	27.3	223	Flavodoxin	2.71
129	Q6FM13	2	27.3	223	Flavodoxin	2.80
130	Q6FM13	3	42.9	316	Flavodoxin	1.03
131	Q6FM13	4	47.5	388	Flavodoxin	0.94
132	Q6FIU4	3	33.7	221	Redoxin	0.76
133	Q6FIU4	4	42.9	288	Redoxin	0.76
134	Q6FIU4	3	33.7	221	Redoxin	0.89
135	Q6FV81	4	39.9	415	Cofilin/tropomyosin-type actin-binding protein	1.13
136	Q6FWL5	4	24.8	191	Copper/zinc superoxide dismutase	0.94
137	Q6FVK5	5	37.7	267	Peptidyl-prolyl cis-trans isomerase	1.08
138	Q6FVK5	5	37.7	267	Peptidyl-prolyl cis-trans isomerase	1.04
139	Q6FYB0	3	33.0	199	60S acidic ribosomal protein	0.57
140	Q6FPF6	5	57.3	424	Heat shock protein 9/12	0.23
1M	Q6FUU4	6	17.4	145	Hexokinase	M[f]

[a]Primary accession numbers from the *Candida glabrata* NCBI blast database (http://www.expasy.org/tools/blast/). [b]Mascot protein score obtained for the protein indicated. Individual protein scores >50 indicate identity or extensive homology ($P < 0.05$). [c]Description of *C. glabrata* or *Saccharomyces cerevisiae* homologous proteins as denoted in the NCBI blast database. [d]Relative amount of the protein spot in the ethidium bromide (ETB)-induced petite mutant compared to its parent isolate (parent isolate/ETB-induced petite mutant). [e]Spots present exclusively in the parent (P) isolate. [f]Spots present exclusively in the ETB-induced petite mutant (M).

coverage, peptide score, and assignment to the strains.

Although most proteins (N = 120) were detected in 2-D gels of both extracts from strains, quantitative changes were shown for some of them. Quadruplicate gel images for each biological sample (at least three protein extracts for each cell type) were obtained and quantitatively analyzed using the ImageMaster 2-D Platinum software to select statistically significant changes ($P < 0.05$, *t*-test). We only considered differences of at least 2-fold in protein expression levels. At least 12 matched spots were higher in the ETB-induced petite mutant (Table 2) and 24 were diminished (Table 2), corresponding to 9 and 11 distinct proteins, respectively. Additionally, some qualitative differences in protein patterns between the two strains were also observed, and the corresponding proteins are listed in Table 3. For example, five proteins involved in carbohydrate degradation, three hexokinases and two glyceraldehyde-3-phosphate dehydrogenases 1 (spots 37-39, 87, 88) were not detected in the cytosolic extract from the ETB-induced petite mutant. Transketolase (spot 85), transaldolase (spot 90), alcohol dehydrogenase (spot 63), inorganic pyrophosphatase (spot 86), and acetyl-coenzyme A synthetase 1 (spots 13-15), also involved in the carbohydrate pathway, were identified only in the parent isolate. The heat shock proteins, Hsp104, Hsp70 and Hsp60 (spots 3-5, 17, and 26, respectively), were exclusive to the parental strain. In contrast, a single hexokinase (spot 1M), which was not detected in the parent isolate, was identified in the ETB-induced petite mutant.

In order to confirm whether some enzymes were essentially decreased in ETB-induced petite mutant, we measured total transketolase, aconitase and catalase activity in both extracts. As expected, we found a significant decrease in enzymatic activity of these three enzymes in the cytosolic extract from the ETB-induced petite mutant ($P < 0.0001$, *t*-test; Table 4).

Discussion

Mechanisms of antifungal resistance in *C. glabrata* are being elucidated at the molecular level. Azole resistance,

Table 2. Spots identified by MS/MS that were higher or lower in the ethidium bromide (ETB)-induced petite mutant compared to parent cells.

Spot	Protein (description)	Function	Abundance change[a]
7,8,9,11	Aconitase	Carbohydrate degradation (citric acid cycle)	↓
24	Transketolase	Pentose-phosphate pathway	↓
33-35	Pyruvate kinase 1	Carbohydrate degradation (glycolysis pathway)	↓
40	Cystathionine beta-synthase domain pair family	Biosynthesis of amino acids	↑
44-46	Catalase	Catalyzes the conversion of hydrogen peroxide to water and molecular oxygen, antioxidant activity	↓
47	ATP synthase beta subunit	ATP synthesis and/or hydrolysis	↓
53	6-Phosphogluconate dehydrogenase	Pentose-phosphate pathway	↓
55	ATP-dependent RNA helicase eIF4A	Translation initiation factor	↑
56	S-adenosylmethionine synthetase	Methionine metabolism	↑
78-80	Transaldolase	Pentose-phosphate pathway	↓
84,91	Glyceraldehyde-3-phosphate dehydrogenase 2	Carbohydrate degradation (glycolysis pathway)	↓
89	Glyceraldehyde-3-phosphate dehydrogenase 1	Carbohydrate degradation (glycolysis pathway)	↑
102,103	WD domain, G-beta repeat family	Involved in diverse functions such as RNA-procession, signal transduction, vesicular trafficking, cytoskeletal assembly, and cell cycle control	↑
107,108	Flavodoxin	Flavin mononucleotide binding	↑
109	Phosphoglycerate mutase	Carbohydrate degradation (glycolysis pathway)	↑
110,111	14-3-3 protein family	Modulates the activity of transcription factors, vesicular transport and cortical actin network organization	↑
112-114	Phosphoglycerate mutase	Carbohydrate degradation (glycolysis pathway)	↓
122	DJ-1/PfpI family	Regulation of RNA-protein interaction, thiamine biosynthesis, Ras-related signal transduction and protease activity	↓
128,129	Flavodoxin	Flavin mononucleotide binding	↓
140	Heat shock protein 9/12	Glucose and lipid-regulated protein	↑

[a]Protein abundance in the ETB-induced petite mutant: ↑ represents higher and ↓ represents lower than in the parent cells.

Table 3. Summary of spots detected only in the parent isolate or its derived ethidium bromide (ETB)-induced petite mutant.

Spot	Protein (description)	Strain	Function
3-5	Heat shock protein 104	Parent isolate	ATPase family associated with various cellular activities
13-15	Acetyl-coenzyme A synthetase 1	Parent isolate	Propanoate and pyruvate metabolism
17	Heat shock protein 70	Parent isolate	Controls signal transducers, promotes regulation of a transcription activator (Hap1)
26	Chaperonin (heat shock protein 60)	Parent isolate	Assembly and disassembly of protein to mitochondria
37-39	Hexokinase	Parent isolate	Carbohydrate degradation (glycolysis pathway)
63	Alcohol dehydrogenase	Parent isolate	Alcohol fermentation pathway
75,76	Flavohemoglobin	Parent isolate	Protect from nitrosative stress
85	Transketolase	Parent isolate	Pentose phosphate pathway
86	Inorganic pyrophosphatase	Parent isolate	Glycogen biosynthetic pathway
87,88	Glyceraldehyde-3-phosphate dehydrogenase 1	Parent isolate	Carbohydrate degradation (glycolysis pathway)
90	Transaldolase	Parent isolate	Link between the glycolytic and pentose-phosphate pathways
115	Unnamed protein product	Parent isolate	-
1M	Hexokinase	ETB-induced mutant	Carbohydrate degradation (glycolysis pathway)

Table 4. Transketolase, aconitase and catalase activities in cytosolic preparations obtained from the parent isolate and the ethidium bromide (ETB)-induced petite mutant.

	Transketolase	Aconitase	Catalase
Parent isolate	13.88 ± 1.4	15.44 ± 1.1	3.13 ± 0.9
ETB-induced petite mutant	7.21 ± 1.53*	7.01 ± 1.1*	1.01 ± 0.35*

Data for transketolase and aconitase are reported as means ± SD and are expressed as ng· min^{-1}·mg $protein^{-1}$. Data for catalase are reported as means ± SD and are expressed as µmol·min^{-1}·mg $protein^{-1}$. *P < 0.0001 compared to the parent isolate (Student *t*-test).

which commonly occurs in patients receiving fluconazole for prophylaxis or therapy, is usually associated with increased mRNA levels of the ATP binding cassette transporters, *CgCDR1*, *CgCDR2* and *PDH1* (16). However, the number of molecular events analyzed in previous studies was usually limited to the overexpression of genes encoding lanosterol demethylase or some efflux pumps and to mutations in the *ERG11* gene. Furthermore, putative changes in other enzymes of the ergosterol pathway were not investigated in most of these studies. The sequencing of the *C. glabrata* genome and recent refinements in protein resolution and identification techniques have greatly enhanced the application of proteomics to the study of this fungal pathogen. Proteome analysis has been applied to studies of virulence, drug response and antifungal resistance in the yeast *C. albicans*. At present, few data are available regarding protein levels in resistant strains of *C. glabrata*. In a laboratory-derived azole-resistant *C. glabrata* isolate, Rogers et al. (27) demonstrated increased levels of the products of the genes *CgCDR1* and *ERG11* using proteome analysis, confirming the up-regulation of these genes. Previous studies from our group and others have revealed that petite mutations, which are caused by the partial or total loss of mitochondrial DNA, are associated with a cross-resistance to almost all the azole drugs due to an increased expression of *CgCDR1* and *CgCDR2* (17,20**)**. Although *CgERG11* expression was not affected in petite mutants, mutant cells showed a marked increase in free ergosterol content (20). The present study was designed to provide additional data using a new methodological approach regarding changes in the expression of nuclear genes induced by the impairment of mitochondrial function. Here, the proteomic analysis of cytosolic proteins of an ETB-induced petite mutant is described and compared to that of the parent strain.

The experiments revealed a huge variety of proteins in the azole-susceptible parent isolate and its derived petite mutant. Changes were observed in the protein pattern in association with the petite mutation, including the low expression of some proteins involved in carbohydrate metabolism. Some of these proteins were identified as aconitase, phosphoglycerate mutase, glyceraldehyde-3-phosphate dehydrogenase 2, and pyruvate kinase 1. Moreover, three isoforms of hexokinase and two of glyceraldehyde-3-phosphate

dehydrogenase were not detected in the ETB-induced mutant. Similarly, a transketolase, a transaldolase and a 6-phosphogluconate dehydrogenase, which play a key role in the regulation of the pentose-phosphate pathway, were down-regulated or not detected in mutant cells. These results suggest a significant decrease in enzymes associated with the metabolic rate of mutant cells aside from the mitochondrial loss, and are therefore in agreement with the limited growth of petite mutants on YEPD agar plates and the increase in the generation time observed in a previous study (22). Although the amount of numerous glycolytic enzymes was lower in mutant cells, an up-regulated isoform of hexokinase was identified, suggesting a possible mechanism of compensation for energy production from glucose.

Sulfur amino acid biosynthesis is peripherally linked to ergosterol biosynthesis. Homocysteine is required for the biosynthesis of *S*-adenosylmethionine, which is necessary for the ability of sterol C-24 methyltransferase to convert zymosterol to fecosterol (28). The up-regulation of cystathionine beta-synthase and *S*-adenosylmethionine synthetase detected in the ETB-mutant may therefore impact the ergosterol biosynthesis pathway in azole resistance, since these enzymes are involved in homocysteine metabolism and *S*-adenosylmethionine synthesis, respectively.

Certain heat shock proteins including Hsp60, Hsp70 and Hsp104, were also shown to be down-regulated or not detected in the ETB-induced mutant. Hsp104, a cytosolic chaperone system member of the AAA+ protein family, is directly involved in the refolding of heat-denatured proteins (29), but full activity of this protein requires cooperation with the Hsp70 chaperone system (30). In 2006, Matsumoto et al. (31) demonstrated that mutant yeasts lacking both the cytosolic Hsp70 genes *SSA1* and *SSA2* presented numerous changes in gene expression with the up-regulation of genes involved in the stress response, protein synthesis and ubiquitin-proteasome protein degradation. A proteome analysis of the yeast strain *ssa1/2* was also carried out and revealed up-regulation of elongation factor eIF-5A proteins and stress-inducible proteins (31). These stress proteins have been shown to play a direct role in the repair of macromolecular complexes involved in the RNA metabolism of yeast cells conditioned to environmental stresses (32).

In *Saccharomyces cerevisiae*, heme, a molecule that indicates oxygen level, binds to and activates Hap1 (33). Hsp70 also promotes regulation of Hap1, required for the activation of aerobic genes (expressed only in the presence of oxygen), including those required for respiration and for the control of oxidative damage, and also indirectly represses hypoxic genes (low-oxygen conditions) by activating *ROX1* (34). Interestingly, among hypoxic genes that are down-regulated in the Hap1-deficient mutant are genes encoding flavohemoglobin and catalase, which are both down-regulated in the petite mutant together with low levels of Hsp70 (35).

Down-regulation of cytosolic Hsp70 in mutant cells is not surprising since they were shown by transmission electron microscopy to be devoid of mitochondria. Indeed, this protein is important for the maintenance of competence for the importation of some mitochondrial precursor proteins (36). The absence of Hsp104 and cytosolic Hsp70 might also lead to a decrease in thermotolerance in petite mutants, which could contribute to their reduced growth rate. Conversely, another heat shock protein, Hsp12, was shown to be up-regulated in mutant cells. Interestingly, in *C. albicans,* the transcriptional factor Tac1p was shown to be responsible not only for the overexpression of the genes *CDR1* and *CDR2*, but also for the up-regulation of other genes including *HSP12* (37). The gene *HSP12* encodes a protein responsible for a shift from the carbohydrate to the lipid metabolism. The present results suggest that *HSP12* overexpression in *C. glabrata* petite mutants, their resistance to azoles and possibly the down-regulation of their carbohydrate metabolism could be regulated by a common transcriptional factor similar to Tac1p. Recently, a zinc-finger protein homologous to Tac1p, called Pdr1p, has been identified in *C. glabrata*, acting as a transcriptional regulator of a pleiotropic drug resistance network (38,39). Disruption of the gene *PDR1* largely reversed azole resistance in azole-resistant isolates with high expression levels of *CDR1* and microarray analysis demonstrated an overexpression of several genes including *HSP12* in a laboratory mutant resistant to fluconazole (40).

Although quite descriptive by having as its main objective the determination of the protein changes induced by petite mutations, the present study provides new insights into the current understanding of the relationships between the impairment of mitochondrial function and azole resistance of petite mutants. The results suggest that regulation of the expression of genes encoding the efflux pumps by certain by-products of mitochondrial metabolism could occur through the regulation of the transcription factors of these genes. Further experiments will be performed to confirm and extend our results by quantifying the expression level of genes encoding up-regulated proteins by PCR, particularly the *HSP12* gene, and to establish the role of the transcription factor Pdr1p in the protein changes observed in mutant cells.

Acknowledgments

The authors are most grateful to Jorge Nascimento Cardoso for excellent technical assistance. We would also like to thank Dr. Gilberto Domont for scientific suggestions and discussions. We are thankful for the use of the MS Platform from the Program for Technological Development of Health Products (PDTIS/FIOCRUZ) and the Proteomic Network of Rio de Janeiro. Research supported by FAPERJ (#E-26/171521/04 and #E-26/171557/06). L.M. Lopes-Bezerra and J. Perales are research fellows of CNPq.

References

1. Carrillo-Munoz AJ, Giusiano G, Ezkurra PA, Quindos G. Antifungal agents: mode of action in yeast cells. *Rev Esp Quimioter* 2006; 19: 130-139.
2. Garcia-Ruiz JC, Amutio E, Ponton J. [Invasive fungal infection in immunocompromised patients]. *Rev Iberoam Micol* 2004; 21: 55-62.
3. Walsh TJ, Groll A, Hiemenz J, Fleming R, Roilides E, Anaissie E. Infections due to emerging and uncommon medically important fungal pathogens. *Clin Microbiol Infect* 2004; 10 (Suppl 1): 48-66.
4. Ruhnke M. Epidemiology of *Candida albicans* infections and role of non-*Candida albicans* yeasts. *Curr Drug Targets* 2006; 7: 495-504.
5. Moran GP, Sullivan DJ, Coleman DC. Emergence of non-*Candida albicans Candida* species as pathogens. In: Calderone RA (Editor), *Candida and candidiasis*. Washington: ASM Press; 2002. p 37-53.
6. Pfaller MA, Diekema DJ, Jones RN, Sader HS, Fluit AC, Hollis RJ, et al. International surveillance of bloodstream infections due to *Candida* species: frequency of occurrence and *in vitro* susceptibilities to fluconazole, ravuconazole, and voriconazole of isolates collected from 1997 through 1999 in the SENTRY antimicrobial surveillance program. *J Clin Microbiol* 2001; 39: 3254-3259.
7. Malani A, Hmoud J, Chiu L, Carver PL, Bielaczyc A, Kauffman CA. *Candida glabrata* fungemia: experience in a tertiary care center. *Clin Infect Dis* 2005; 41: 975-981.
8. Pfaller MA, Diekema DJ. Twelve years of fluconazole in clinical practice: global trends in species distribution and fluconazole susceptibility of bloodstream isolates of *Candida*. *Clin Microbiol Infect* 2004; 10 (Suppl 1): 11-23.
9. Panackal AA, Gribskov JL, Staab JF, Kirby KA, Rinaldi M, Marr KA. Clinical significance of azole antifungal drug cross-resistance in *Candida glabrata*. *J Clin Microbiol* 2006; 44: 1740-1743.
10. Sanguinetti M, Posteraro B, Fiori B, Ranno S, Torelli R, Fadda G. Mechanisms of azole resistance in clinical isolates of *Candida glabrata* collected during a hospital survey of antifungal resistance. *Antimicrob Agents Chemother* 2005; 49: 668-679.
11. Khan ZU, Ahmad S, Al-Obaid I, Al-Sweih NA, Joseph L, Farhat D. Emergence of resistance to amphotericin B and triazoles in *Candida glabrata* vaginal isolates in a case of recurrent vaginitis. *J Chemother* 2008; 20: 488-491.
12. Charlier C, Hart E, Lefort A, Ribaud P, Dromer F, Denning DW, et al. Fluconazole for the management of invasive candidiasis: where do we stand after 15 years? *J Antimicrob Chemother* 2006; 57: 384-410.
13. Sanglard D, Bille J. Current understanding of the modes of action and resistance mechanisms to conventional and emerging antifungal agents for treatment of *Candida* infections. In: Calderone RA (Editor), *Candida and candidiasis*. Washington: ASM Press; 2002. p 349-383.
14. Franz R, Kelly SL, Lamb DC, Kelly DE, Ruhnke M, Morschhauser J. Multiple molecular mechanisms contribute to a stepwise development of fluconazole resistance in clinical *Candida albicans* strains. *Antimicrob Agents Chemother* 1998; 42: 3065-3072.
15. Sanglard D, Ischer F, Parkinson T, Falconer D, Bille J. *Candida albicans* mutations in the ergosterol biosynthetic pathway and resistance to several antifungal agents. *Antimicrob Agents Chemother* 2003; 47: 2404-2412.
16. Bennett JE, Izumikawa K, Marr KA. Mechanism of increased fluconazole resistance in *Candida glabrata* during prophylaxis. *Antimicrob Agents Chemother* 2004; 48: 1773-1777.
17. Sanglard D, Ischer F, Calabrese D, Majcherczyk PA, Bille J. The ATP binding cassette transporter gene CgCDR1 from *Candida glabrata* is involved in the resistance of clinical isolates to azole antifungal agents. *Antimicrob Agents Chemother* 1999; 43: 2753-2765.
18. Sanglard D, Ischer F, Bille J. Role of ATP-binding-cassette transporter genes in high-frequency acquisition of resistance to azole antifungals in *Candida glabrata*. *Antimicrob Agents Chemother* 2001; 45: 1174-1183.
19. Brun S, Aubry C, Lima O, Filmon R, Berges T, Chabasse D, et al. Relationships between respiration and susceptibility to azole antifungals in *Candida glabrata*. *Antimicrob Agents Chemother* 2003; 47: 847-853.
20. Brun S, Berges T, Poupard P, Vauzelle-Moreau C, Renier G, Chabasse D, et al. Mechanisms of azole resistance in petite mutants of *Candida glabrata*. *Antimicrob Agents Chemother* 2004; 48: 1788-1796.
21. Traven A, Wong JM, Xu D, Sopta M, Ingles CJ. Interorganellar communication. Altered nuclear gene expression profiles in a yeast mitochondrial DNA mutant. *J Biol Chem* 2001; 276: 4020-4027.
22. Brun S, Dalle F, Saulnier P, Renier G, Bonnin A, Chabasse D, et al. Biological consequences of petite mutations in *Candida glabrata*. *J Antimicrob Chemother* 2005; 56: 307-314.
23. Rabilloud T. Use of thiourea to increase the solubility of membrane proteins in two-dimensional electrophoresis. *Electrophoresis* 1998; 19: 758-760.
24. Bjellqvist B, Sanchez JC, Pasquali C, Ravier F, Paquet N, Frutiger S, et al. Micropreparative two-dimensional electrophoresis allowing the separation of samples containing milligram amounts of proteins. *Electrophoresis* 1993; 14: 1375-1378.
25. Pitarch A, Sanchez M, Nombela C, Gil C. Sequential fractionation and two-dimensional gel analysis unravels the complexity of the dimorphic fungus *Candida albicans* cell wall proteome. *Mol Cell Proteomics* 2002; 1: 967-982.
26. Aebi H. Catalase *in vitro*. *Methods Enzymol* 1984; 105: 121-126.
27. Rogers PD, Vermitsky JP, Edlind TD, Hilliard GM. Proteomic analysis of experimentally induced azole resistance in *Candida glabrata*. *J Antimicrob Chemother* 2006; 58: 434-438.
28. De Backer MD, Ilyina T, Ma XJ, Vandoninck S, Luyten WH, Vanden Bossche H. Genomic profiling of the response of *Candida albicans* to itraconazole treatment using a DNA microarray. *Antimicrob Agents Chemother* 2001; 45: 1660-1670.
29. Seppa L, Makarow M. Regulation and recovery of functions of *Saccharomyces cerevisiae* chaperone BiP/Kar2p after thermal insult. *Eukaryot Cell* 2005; 4: 2008-2016.
30. Bosl B, Grimminger V, Walter S. The molecular chaperone Hsp104 - a molecular machine for protein disaggregation. *J Struct Biol* 2006; 156: 139-148.
31. Matsumoto R, Rakwal R, Agrawal GK, Jung YH, Jwa NS,

Yonekura M, et al. Search for novel stress-responsive protein components using a yeast mutant lacking two cytosolic Hsp70 genes, SSA1 and SSA2. *Mol Cells* 2006; 21: 381-388.
32. Bond U. Stressed out! Effects of environmental stress on mRNA metabolism. *FEMS Yeast Res* 2006; 6: 160-170.
33. Hon T, Dodd A, Dirmeier R, Gorman N, Sinclair PR, Zhang L, et al. A mechanism of oxygen sensing in yeast. Multiple oxygen-responsive steps in the heme biosynthetic pathway affect Hap1 activity. *J Biol Chem* 2003; 278: 50771-50780.
34. Hickman MJ, Winston F. Heme levels switch the function of Hap1 of *Saccharomyces cerevisiae* between transcriptional activator and transcriptional repressor. *Mol Cell Biol* 2007; 27: 7414-7424.
35. Ter Linde JJ, Steensma HY. A microarray-assisted screen for potential Hap1 and Rox1 target genes in *Saccharomyces cerevisiae*. *Yeast* 2002; 19: 825-840.
36. Asai T, Takahashi T, Esaki M, Nishikawa S, Ohtsuka K, Nakai M, et al. Reinvestigation of the requirement of cytosolic ATP for mitochondrial protein import. *J Biol Chem* 2004; 279: 19464-19470.
37. Coste AT, Karababa M, Ischer F, Bille J, Sanglard D. TAC1, transcriptional activator of CDR genes, is a new transcription factor involved in the regulation of *Candida albicans* ABC transporters CDR1 and CDR2. *Eukaryot Cell* 2004; 3: 1639-1652.
38. Vermitsky JP, Edlind TD. Azole resistance in *Candida glabrata*: coordinate upregulation of multidrug transporters and evidence for a Pdr1-like transcription factor. *Antimicrob Agents Chemother* 2004; 48: 3773-3781.
39. Tsai HF, Krol AA, Sarti KE, Bennett JE. *Candida glabrata* PDR1, a transcriptional regulator of a pleiotropic drug resistance network, mediates azole resistance in clinical isolates and petite mutants. *Antimicrob Agents Chemother* 2006; 50: 1384-1392.
40. Vermitsky JP, Earhart KD, Smith WL, Homayouni R, Edlind TD, Rogers PD. Pdr1 regulates multidrug resistance in *Candida glabrata*: gene disruption and genome-wide expression studies. *Mol Microbiol* 2006; 61: 704-722.